

Orbital excitations in titanates

C. Ulrich,¹ A. Gössling,² M. Grüninger,² M. Guennou,¹
H. Roth,² M. Cwik,² T. Lorenz,² G. Khaliullin,¹ and B. Keimer¹

¹*Max-Planck-Institut für Festkörperforschung, Heisenbergstr. 1, D-70569 Stuttgart, Germany*

²*II. Physikalisches Institut, Universität zu Köln, 50937 Köln, Germany*

(Dated: November 26, 2018)

Raman scattering is used to observe pronounced electronic excitations around 230 meV – well above the two-phonon range – in the Mott insulators LaTiO₃ and YTiO₃. Based on the temperature, polarization, and photon energy dependence, the modes are identified as orbital excitations. The observed profiles bear a striking resemblance to magnetic Raman modes in the insulating parent compounds of the superconducting cuprates, indicating an unanticipated universality of the electronic excitations in transition metal oxides.

PACS numbers: 78.30.Hv, 71.28.+d, 75.50.Ee, 75.50.Dd

Transition metal oxides with orbital degeneracy exhibit a host of intriguing physical properties, such as “colossal magnetoresistance” in manganites or unconventional superconductivity in ruthenium oxides [1, 2]. Collective oscillations of the valence electrons between different atomic orbitals (termed “orbitons”) contain a wealth of information about the microscopic interactions underlying this behavior. Experiments introducing Raman scattering as a direct probe of orbitons in LaMnO₃ have hence opened up new perspectives for a quantitative understanding of colossal magnetoresistance [3]. The results, however, have proven to be quite controversial, because the modes observed in LaMnO₃ are difficult to discriminate from ordinary two-phonon excitations [4, 5].

Insulating titanates such as LaTiO₃ and YTiO₃ have only one valence electron residing on the Ti³⁺ ions. Despite their similar, nearly cubic lattice structures, the magnetic ground states of LaTiO₃ and YTiO₃ are quite different: Whereas LaTiO₃ orders antiferromagnetically at T_N ~ 150 K, YTiO₃ is a ferromagnet with Curie temperature T_C ~ 30 K. The origin of this difference lies in the large degeneracy of the quantum states available to the valence electron. In addition to its spin degeneracy, this electron can occupy any combination of the three *t*_{2g}-orbitals *xy*, *xz* and *yz*. The six single-ion states on neighboring sites are coupled by the superexchange interaction and collective lattice distortions, which generate a plethora of nearly degenerate many-body states with different spin and orbital ordering patterns.

The mechanisms selecting the ground state out of this large manifold of states have recently been a focus of intense research. Two theoretical approaches have emerged. According to point charge model [6, 7, 8], band structure [9, 10] and LDA-DMFT [11] calculations, the degeneracy of the single-ion *t*_{2g}-levels is lifted by subtle lattice distortions. These distortions favor linear combinations of type $(xz + yz + xy)/\sqrt{3}$ for LaTiO₃ and a staggered pattern of planar orbitals of the kind $(xz + xy)/\sqrt{2}$ in YTiO₃. This proposal has received support from NMR [12, 13] and neutron diffraction [14] experiments. How-

ever, the small ordered moment and some aspects of the low-temperature spin excitation spectra, such as their spatial isotropy and small gaps, are difficult to reconcile with the scenario of static, lattice-driven orbital order [15, 16]. An alternative theoretical approach [17, 18] inspired by these findings emphasizes the collective quantum dynamics of the orbitals, driven by intersite correlations via the superexchange interaction. Frustrations inherent to these interactions give rise to strong quantum fluctuations that suppress orbital ordering and stabilize more isotropic charge distributions around the Ti³⁺ ions.

Orbital excitations have the potential to discriminate between these conflicting scenarios. When the orbital dynamics is quenched by lattice distortions, one expects a number of transitions between well-defined crystal field levels, with selection rules dictated by the symmetry of these distortions. The picture is similar to the local crystal field excitations of, e.g., Ti³⁺ impurities in a distorted corundum lattice [19]. In an orbitally fluctuating state, on the other hand, the orbital excitations are collective modes with selection rules controlled by many-body effects and hence are very different from local crystal field excitations. Therefore, the observation of orbital excitations and comparison of their properties in YTiO₃ and LaTiO₃, two materials with different lattice distortions and magnetic ground states, is of crucial importance for the understanding of this hotly debated issue.

We have used Raman scattering to search for orbital excitations in LaTiO₃ and YTiO₃. The samples were high quality single crystals with T_N = 146 K and T_C = 27 K, respectively, grown by the floating zone technique described in Ref. [6]. The LaTiO₃ crystal was partly twinned. Raman measurements were performed using a Dilor-XY triple spectrometer equipped with a CCD-detector. The measured spectral intensity was calibrated by using a white light source (Ulbricht-sphere) as reference. Different lines of an Ar⁺/Kr⁺ mixed-gas ion laser were used. In order to avoid heating of the sample, the power of the incident laser beam was kept below 10 mW at the sample position. The experiments

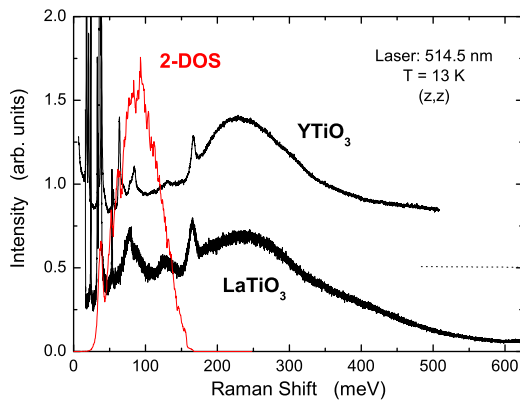


FIG. 1: Raman spectra of LaTiO₃ and YTiO₃ measured at T = 13 K using the 514.5 nm laser line in (z, z) polarization. The red line shows the calculated two-phonon density of states.

were performed in backscattering geometry parallel to the crystallographic *b*-direction (within the *Pbnm* space group). The polarizations of the incident and scattered photons are specified as (α, β) where α and β denote the z, x, z' or x' directions. Note that $z \parallel c$ is along the nearest-neighbor Ti–Ti bond whereas x is along the next-nearest-neighbor Ti–Ti direction in the *ab*-plane. The z' and x' directions are rotated by 45° from z and x .

Figure 1 shows the Raman spectra of LaTiO₃ and YTiO₃ over a wide energy range. Up to 80 meV, the spectra are dominated by one-phonon excitations reported before [20, 21]. A series of weak features extends up to 170 meV. At still higher frequencies, around 235 meV, a pronounced broad peak is observed in both compounds. The latter feature has hitherto not been reported and constitutes the central observation of this paper.

In order to establish whether the broad peak can be attributed to two-phonon excitations, we have evaluated the two-phonon density of states (2-DOS) of YTiO₃ by convoluting the one-phonon dispersion curves calculated within a shell model whose parameters were fitted to the observed phonon frequencies [22]. The 2-DOS, responsible for the weak features between 80 and 170 meV, terminates at about 170 meV. The broad peak thus occurs well above the two-phonon spectral range, in contrast to the features around 160 meV discussed for LaMnO₃ [3, 4]. Since higher phonon orders are expected to appear even weaker, lattice vibrations can be ruled out as the origin of the high-energy Raman peak. As an aside, we note the presence of a sharp feature at the upper edge of the 2-DOS around 165 meV, which is not reproduced by our calculation. This peak is also observed by inelastic neutron scattering [22]. A similar Raman mode is also observed in other transition metal oxides [3, 20, 23, 25], and has been attributed to a two-phonon excitation [4, 20, 23, 25].

In order to rule out photoluminescence as a cause of the broad peak, we have repeated the Raman measurements

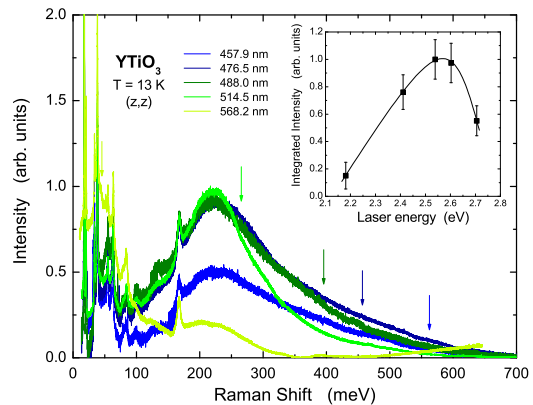


FIG. 2: Raman spectrum of YTiO₃ measured at T = 13 K for different laser lines. A frequency independent background has been subtracted from every profile. The arrows depict the position of the photoluminescence peak at 2.14 eV for the different laser lines. The inset shows the integrated intensity of the broad high-energy peak.

with different laser lines between 457.9 nm and 568.2 nm (Fig. 2). The peak at 235 meV does not shift as the laser frequency is changed, ruling out photoluminescence as origin and demonstrating that the peak position corresponds to a genuine excitation frequency. The data also show the manifestations of a weak photoluminescence feature of energy 2.14 eV and width 75 meV, which is responsible for the low-energy intensity in the data at the laser wavelength 568.2 nm. Since the Raman spectra are measured at energy transfers relative to the incident laser energy, the luminescence peak is shifted when the laser energy is changed and contributes to the variation of the apparent lineshape of the 235 meV mode with laser wavelength. However, the main part of the mode profile is unaffected by this extraneous feature. The inset of Figure 2 shows that the integrated spectral weight of the 235 meV mode in YTiO₃ exhibits a pronounced resonant enhancement at a laser frequency of ~ 2.54 eV. The Raman spectra displayed in Figure 3 demonstrate that its spectral weight is also strongly temperature dependent, decreasing continuously with increasing temperature.

The intensity of the mode depends strongly on the light polarization (Fig. 4). In a cubic crystal, the Raman intensity for parallel and crossed polarizations can be expressed via E_g, T_{2g} and A_{1g} symmetry components:

$$I_{parallel} = \left(\frac{2}{3} - a_\theta - b_\theta\right)E_g + (a_\theta + b_\theta)T_{2g} + \frac{1}{3}A_{1g},$$

$$I_{crossed} = b_\theta E_g + \left(\frac{1}{2} - b_\theta\right)T_{2g}, \quad (1)$$

where θ is the angle between the incident electric field vector and the *c*-axis, $a_\theta = \frac{1}{2}\sin^2\theta$, $b_\theta = \frac{3}{8}\sin^2 2\theta$, and $\theta = 90^\circ$ corresponds to the *a* (or *b*) axis. These relations provide a good description of the observed polarization dependences in both compounds (insets in Fig. 4). Possible corrections induced by lattice distortions away from

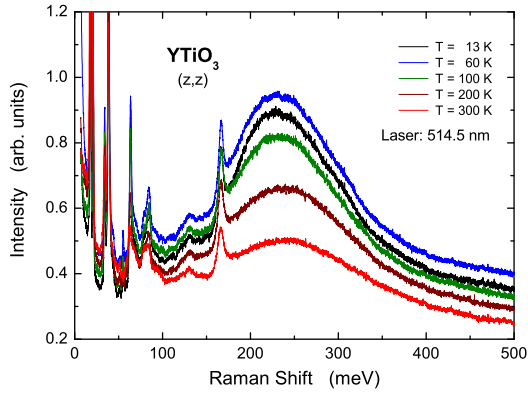


FIG. 3: Temperature dependence of the Raman spectrum of YTiO_3 in (z, z) geometry, using the 514.5 nm laser line.

cubic symmetry therefore appear to be rather small. The observed nearly cubic symmetry of the high-energy Raman response is in accord with the cubic symmetry of spin wave dispersions in these compounds [15, 16].

We now turn to the interpretation of the 235 meV mode. Having ruled out phonons and photoluminescence, we attribute the mode to electronic scattering. Its line-shape, temperature, and polarization dependence shows striking similarities (elaborated later on) with the Raman scattering from spin-pair excitations in the insulating parent compounds of the superconducting cuprates [23, 24, 25]. However, a simple two-magnon origin of the broad band is ruled out here because YTiO_3 is ferromagnetic, and because the peak energy is much higher than twice the magnon energies found by neutron scattering: ~ 20 meV in YTiO_3 [16] and ~ 44 meV in LaTiO_3 [15]. We thus attribute the broad Raman mode to the orbital degrees of freedom of the valence electron.

Let us start with a simple crystal field picture where the incident photon excites an oxygen $2p$ electron to unoccupied t_{2g} -orbitals via the charge-transfer gap Δ_{pd} and, in a second step, the d -electron in the ground state orbital relaxes to the oxygen site emitting a photon and leaving a “flipped” orbital behind. Predictions for the energy cost of such a local orbital flip vary between 27 and 240 meV [6, 10, 11], but some model calculations yield energies comparable to those observed experimentally [6]. The large width of the crystal field transitions can be understood as a consequence of coupling to lattice vibrations. Other aspects of the Raman data are, however, difficult to reconcile with a local crystal field scenario. First, the experimentally observed strong temperature dependence of the spectral weight is hard to understand within this picture, as the local pd charge transfer process is not sensitive to temperature variations. Second, the above described scenario cannot explain the observed strong resonance at a photon energy of 2.54 eV, which is far below the pd -excitation energy $\Delta_{pd} > 4$ eV [26].

The resonance energy yields an important clue to the

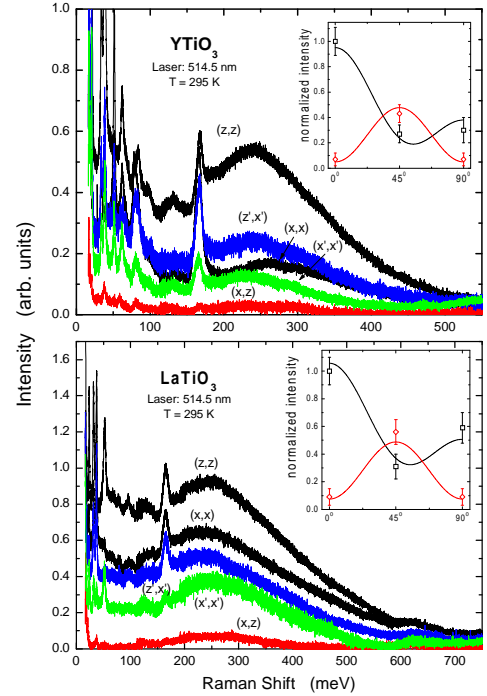


FIG. 4: Polarization dependences of the Raman spectra of YTiO_3 and LaTiO_3 at room temperature. The intensity is symmetric with respect to $(\alpha, \beta) \rightarrow (\beta, \alpha)$. A frequency independent background has been subtracted. Insets: scattering intensities for the parallel (\square) and crossed (\diamond) polarizations as function of angle θ . Solid and dashed lines are obtained from Eq. (1), with relative intensities $E_g : A_{1g} : T_{2g} \approx 1 : 0.3 : 0.1$ ($1 : 0.5 : 0.1$) in YTiO_3 (LaTiO_3).

microscopic origin of the broad Raman peak. As it falls in the range of intersite $d_i \rightarrow d_j$ excitations in optical spectra [26], *two* Ti sites must be involved in the Raman process. This means that the t_{2g} -electron is first transferred to a neighboring site by the incident photon that matches the $d_i \rightarrow d_j$ transition energy. The intermediate state then relaxes back, leaving behind flipped orbitals either on one or on both sites, depending on the actual orbital pattern. Consider again the lattice-driven orbital picture, where detailed predictions are available [27]. According to these predictions, the orbital excitations probed by light polarized along different crystal axes are fundamentally different. In particular, the selection rules for the four-sublattice pattern $(xz \pm xy)/\sqrt{2}$, $(yz \pm xy)/\sqrt{2}$ suggested for YTiO_3 [9, 12, 14] allow a single orbital-flip for ab -plane polarization, but only two-orbiton excitations may occur in case of light polarization along the c -axis [27]. This selection rule (which results from a mirror symmetry of the Ti-O-Ti bonds along the c -axis) is in sharp contrast with the observed nearly cubic selection rules. Similar considerations can be made for the orbital state proposed for LaTiO_3 .

The insensitivity of the orbiton excitations to details of the lattice distortions suggests that electronic interactions play a major part in driving the orbital state,

as proposed in Refs. [15, 16, 17, 18]. In this picture, the orbitals are regarded as quantum objects much like the spins of the correlated electrons, and interact with each other via the superexchange mechanism. The superexchange originates from virtual charge fluctuations representing the residual kinetic energy of electrons in a Mott insulator. Similar to the spin exchange (permutation) operator $\hat{P}_s = (2\vec{s}_i\vec{s}_j + \frac{1}{2}n_in_j)$, the orbital exchange is described by $\hat{P}_{orb} = (2\vec{\tau}_i\vec{\tau}_j + \frac{1}{2}n_in_j)^{(\gamma)}$, where the action of pseudospins $\vec{\tau}^{(\gamma)}$ on the t_{2g} orbital triplet depends on the bond direction γ , leading to strong frustration of orbitals on a cubic lattice [17, 18]. These frustrations, as well as the simultaneous spin/orbital exchange described by a product $\hat{P}_s\hat{P}_{orb}$, result in a large degeneracy of competing many-body states, including the near-degeneracy of spin ferro- and antiferromagnetic states. The high-energy response of orbitals in titanates is governed by the universal scale $J_{SE} \propto 4t^2/U_{dd}$ (*per bond*), controlled by the kinetic energy t and Hubbard correlation U_{dd} . Weak lattice distortions tend to polarize the many-body orbital state, but the high-energy orbital fluctuations respect the nearly cubic symmetry of the electronic ground state. This mechanism has also been invoked to explain the isotropic spin-wave spectra [15, 16].

In the superexchange-driven orbital state of YTiO₃ [18], the light scattering from fluctuations of the *orbital-exchange* bonds, described by \hat{P}_{orb} , leads to a two-orbital Raman band of cubic E_g symmetry [28], as observed. The A_{1g} and T_{2g} components are explained due to next-nearest-neighbor orbital exchange terms that are enhanced by resonant scattering, in complete analogy to the theory of magnetic Raman scattering in the cuprates [29]. From an analysis of the spin-wave data of Ref. [16], the highest orbital energy was determined as $\sim 2r_1J_{SE}$ with $r_1J_{SE} \sim 60$ meV and $r_1 \sim 1.5$ [18], in reasonable agreement with a two-orbital peak at the experimental value of 235 meV.

Since the orbital excitations are strongly damped because of frustrating interactions, their response is broad in both momentum and energy, as observed. The strong enhancement of the peak intensity at low temperature can be understood if the intermediate electronic state involved in the resonant Raman process has high-spin configuration. The relevant matrix element is thus controlled by intersite spin correlations via the operator $(\vec{s}_i\vec{s}_j + \frac{3}{4})$, selecting a triplet state. The square of this quantity changes by roughly factor of two between the high and low temperature limits, consistent with the experiment.

In summary, the high-energy orbital excitations in LaTiO₃ and YTiO₃ are quite insensitive to distortions of the lattice away from cubic symmetry. The superexchange-driven quantum orbital picture provides a consistent description of this observation as well as the polarization and temperature dependence of these excitations. In this picture, the high-energy Raman peak is due to light scattering from exchange-bond fluctuations,

a process which is basically identical to magnetic Raman scattering in copper oxides. A pseudospin-like behaviour of quantum orbitals explains why the Raman response of two apparently different degrees of freedom exhibit very similar features. In fact, the energies of the two-orbital Raman mode in the titanates (~ 235 meV) and the two-magnon mode in the cuprates (~ 350 meV) are related by the simple scaling relation for the exchange-pair energy $\Omega_{pair} \sim (z-1)J_{SE}$, where J_{SE} and z are the strength and number of exchange bonds, respectively. These considerations, which can be readily extended to other transition metal compounds with more than one valence electron (or hole), provide a glimpse of an underlying universality in the electronic spectra of these complex materials.

We would like to thank M. Cardona, R. Zeyher, and R. Rückamp for useful discussions.

-
- [1] M. Imada, A. Fujimori, and Y. Tokura, Rev. Mod. Phys. **70**, 1039 (1998).
 - [2] Y. Tokura and N. Nagaosa, Science **288**, 462 (2000).
 - [3] E. Saitoh *et al.*, Nature **410**, 180 (2001).
 - [4] M. Grüninger *et al.*, Nature **418**, 39 (2002).
 - [5] E. Saitoh *et al.*, Nature **418**, 40 (2002).
 - [6] M. Cwikel *et al.*, Phys. Rev. B **68**, 060401(R) (2003).
 - [7] M. Mochizuki and M. Imada, Phys. Rev. Lett. **91**, 167203 (2003).
 - [8] R. Schmitz *et al.*, cond-mat/0411583.
 - [9] H. Sawada, N. Hamada, and K. Terakura, Physica B **237-238**, 46 (1997).
 - [10] I.V. Solov'ev, Phys. Rev. B **69**, 134403 (2004).
 - [11] E. Pavarini *et al.*, Phys. Rev. Lett. **92**, 176403 (2004).
 - [12] M. Itoh, M. Tsuchiya, H. Tanaka, and K. Motoya, J. Phys. Soc. Jpn. **68**, 2783 (1999).
 - [13] T. Kiyama and M. Itoh, Phys. Rev. Lett. **91**, 167202 (2003).
 - [14] J. Akimitsu *et al.*, J. Phys. Soc. Jpn. **70**, 3475 (2001).
 - [15] B. Keimer *et al.*, Phys. Rev. Lett. **85**, 3946 (2000).
 - [16] C. Ulrich *et al.*, Phys. Rev. Lett. **89**, 167202 (2002).
 - [17] G. Khaliullin and S. Maekawa, Phys. Rev. Lett. **85**, 3950 (2000); G. Khaliullin, Phys. Rev. B **64**, 212405 (2001).
 - [18] G. Khaliullin and S. Okamoto, Phys. Rev. Lett. **89**, 167201 (2002); Phys. Rev. B **68**, 205109 (2003).
 - [19] E.D. Nelson, J.Y. Wong, and A.L. Schawlow, Phys. Rev. **156**, 298 (1967).
 - [20] M. Reedyk *et al.*, Phys. Rev. B **55**, 1442 (1997).
 - [21] M.N. Iliev *et al.*, Phys. Rev. B **69**, 172301 (2004).
 - [22] C. Ulrich *et al.*, to be published.
 - [23] K.B. Lyons, P.A. Fleury, L.F. Schneemeyer, and J.V. Waszczak, Phys. Rev. Lett. **60**, 732 (1988).
 - [24] P. Knoll, C. Thomsen, M. Cardona, and P. Murugaraj, Phys. Rev. B **42**, R4842 (1990).
 - [25] M. Yoshida *et al.*, Phys. Rev. B **46**, 6505 (1992).
 - [26] Y. Okimoto *et al.*, Phys. Rev. B **51**, 9581 (1995).
 - [27] S. Ishihara, Phys. Rev. B **69**, 075118 (2004).
 - [28] G. Khaliullin, to be published.
 - [29] B.S. Shastry and B.I. Shraiman, Phys. Rev. Lett. **65**, 1068 (1990).